Noninvasive Acoustic Measurements in Cylindrical Shell Containers

John Greenhall, *Member, IEEE*, Christopher Hakoda, *Member, IEEE*, Eric S. Davis, *Member, IEEE*, Vamshi Krishna Chillara, *Senior Member, IEEE*, and Cristian Pantea, *Senior Member, IEEE*

***Abstract*— Acoustic time-of-flight (ToF) measurements enable noninvasive material characterization, acoustic imaging, and defect detection and are commonly used in industrial process control, biomedical devices, and national security. When characterizing a fluid contained in a cylinder or pipe, ToF measurements are hampered by guided waves, which propagate around the cylindrical shell walls and obscure the waves propagating through the interrogated fluid. We present a technique for overcoming this limitation based on a broadband linear chirp excitation and cross correlation detection. By using broadband excitation, we exploit the dispersion of the guided waves, wherein different frequencies propagate at different velocities, thus distorting the guided wave signal while leaving the bulk wave signal in the fluid unperturbed. We demonstrate the measurement technique experimentally and using numerical simulation. We characterize the technique performance in terms of measurement error, signal-to-noise-ratio, and resolution as a function of the linear chirp center frequency and bandwidth. We discuss the physical phenomena behind the guided bulk wave interactions and how to utilize these phenomena to optimize the measurements in the fluid.**

***Index Terms*— Guided wave dispersion, nondestructive evaluation, noninvasive acoustic measurement.**

I. Introduction

NONINVASIVE acoustic identification or classification of materials is of great interest in a wide range of applications. This includes chemical or biological weapons' classification [1], where invasive techniques pose a potential safety hazard; *in situ* process control [2], where existing techniques can incur great cost; or chemical reaction monitoring [3], where acoustics provide information not available via other techniques. Active acoustic characterization techniques are typically categorized as either frequency-domain or time-domain techniques. Frequency-domain techniques excite the specimen at a specific frequency and measure the resulting amplitude of vibration in the specimen. Repeating this measurement for a range of frequencies provides the frequency response of the system. Resonant ultrasound spectroscopy [4], [5] and swept-frequency acoustic interferometry [6] achieve these frequency-domain measurements in structures and fluids, respectively, by exciting and measuring the vibrations via contact transducers. Alternatively, frequency-domain measurements have been achieved for submerged structures via noncontact excitation and measurement using techniques known as vibro-acoustography and resonance scattering. The vibro-acoustography enables measuring the resonances of a submerged structure in a noncontact manner by exciting the structure with acoustic radiation force and then measuring the acoustic emission from the structure [7], [8]. Resonance scattering has been demonstrated for measuring the resonances of submerged structures by transmitting a plane acoustic wave and then measuring the wave that scatters from the submerged structure [9], [10]. The resulting frequency response is rich in data about the system resonances and can provide information such as the shear and longitudinal sound speed, density, and acoustic attenuation. However, determining which frequency components correspond to each physical component (fluid specimen, container, or transmitter/receiver) can be challenging. Additionally, geometries or materials with low-quality factors can inhibit the detection of different features in the frequency response due to the overlap between resonance peaks [11]. For resonance-scattering techniques, the scattered wave consists of a radiated component that contains information about the structure resonances and a specular component that obscures the radiated component. Thus, the radiated component must be isolated by subtracting the specular component, which can be estimated analytically [12], [13]. Additionally, resonant modes can be identified based on "jumps" in the phase of the frequency response [14]. These techniques are effective for identifying resonance peaks in cylindrical shell structures with high-quality factors, but not for fluids within the cylindrical shells, which tend to be more attenuating. Rembert *et al.* [15] demonstrated a resonance-scattering technique for measuring water resonances within a cylindrical shell, but the technique requires measuring the scattered wave from a wide range of angles around the cylinder, which complicate implementation, and the technique may not work for more highly attenuating fluids.

Alternatively, time-domain techniques use an acoustic burst that propagates through the container and interacts with the specimen. Time-domain techniques typically use either a "pitch-catch" configuration, where the acoustic burst propa-

Manuscript received December 14, 2020; accepted January 21, 2021. Date of publication January 26, 2021; date of current version May 25, 2021. This work was supported by the U.S. Department of Energy under Grant 89233218CNA000001. *(Corresponding author: John Greenhall.)*

The authors are with Materials Physics and Applications, Los Alamos National Laboratory, Los Alamos, NM 87545, USA (e-mail: jgreenhall@lanl.gov).

Digital Object Identifier 10.1109/TUFFC.2021.3054716

gates from a transmitter through the specimen and is then measured by an opposing receiver, or a "pulse-echo" configuration, where the acoustic burst propagates from a transmitter through the specimen and then reflects back to the transmitter. In either configuration, the time-of-flight (ToF) T_b is measured to calculate either the specimen sound speed c or size l based on the simple equation $T_b = nl/c$, where $n = 1$ for pitch-catch and $n = 2$ for pulse-echo measurements. Time-domain techniques do not typically provide the same level of measurement accuracy as frequency-domain techniques, but they also do not require a high-quality factor specimen, they work for more complicated geometries, and they utilize only basic signal processing. Specifically, time-domain techniques require measuring the arrival time of the acoustic burst, which is a well-understood problem in estimation theory [16].

ToF measurement is efficient and simple to implement when the measured signal contains a single burst. However, in the case of noninvasive measurements of a fluid within a cylindrical shell, the acoustic burst propagates simultaneously through the fluid in the form of a bulk wave and through the walls of the cylindrical shell in the form of circumferential guided waves. Within the cylindrical shell wall, the burst can excite multiple guided wave modes, each with a different arrival time, based on the mode and excitation frequency. Frequently, these guided waves will overlap with the bulk wave, which inhibits identifying the bulk wave arrival time, and thus, introduces significant error in the acoustic measurement. Guided wave propagation has been studied extensively in the literature [17]–[23]. However, separating the contributions of the guided waves from one another or from the bulk wave is challenging and currently an open problem [24]. In practice, acoustic measurements within the cylindrical shells typically rely on a time-separation between the guided wave and the bulk wave arrivals [25] or rely on nonlinear interactions within a flowing fluid [2]. In general, the guided wave and the bulk wave arrivals cannot be separated temporally, and the material in the cylindrical shell may not be flowing. Thus, to overcome the guided wave interference, broadband chirp signals have been previously implemented [26], [27]. Recently, Chillara *et al.* [27] reported on a technique to enable measuring bulk wave arrivals in the presence of guided waves in a cylindrical shell. The technique first measures a baseline signal containing only the guided wave signal by introducing gas into the fluid to completely attenuate the bulk wave, while leaving enough liquid to still achieve wetting of the inside wall. In subsequent measurements, the bulk wave can be isolated by subtracting the baseline signal from the measurement. One critical finding was that simply measuring the baseline with an empty cylindrical shell was not sufficient due to the interactions between the liquid and the cylindrical shell. However, in many applications, it is not feasible to introduce gas into the fluid to measure the baseline signal. To our knowledge, there is currently no analysis in the literature of how the frequency content of the broadband excitation signal affects ToF measurements in a cylindrical shell. As a result, there is a significant gap in the literature on noninvasive acoustic measurements within the cylindrical shells such as pipes, tubes, and vats.

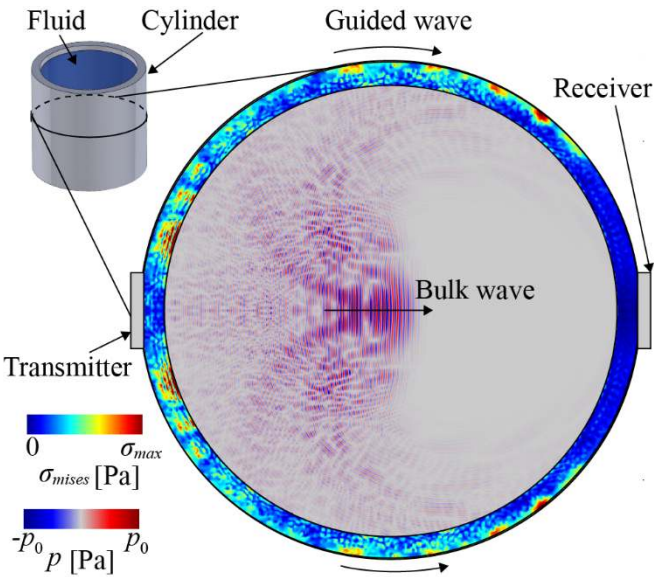

Fig. 1. Noninvasive acoustic measurement within a closed cylindrical shell. A time snapshot depicts the bulk and guided waves as they propagate from the transmitter.

Thus, the objective of this work is to present a noninvasive time-domain ultrasound technique to measure the sound speed of a fluid within a closed cylindrical container based on the linear chirp acoustic excitation. A theoretical basis for the technique is presented and validated experimentally on a water-filled cylindrical shell. We characterize the ToF error, signal-to-noise ratio (SNR), and measurement resolution as a function of the center frequency and bandwidth of the linear chirp excitation. As a result, this work provides guidelines for performing accurate and reliable noninvasive acoustic characterization of a fluid within a closed cylindrical shell.

II. Guided and Propagating Waves in Fluid-Filled Cylindrical Shells

Fig. 1 shows a schematic of the fluid-filled cylindrical shell of inner diameter $2a$, outer diameter $2b$, and wall thickness $h = b\text{-}a$ with opposing transmitter/receiver ultrasound transducers mounted to the cylindrical shell exterior. We excite the transmitter with a burst that generates an acoustic wave, which propagates from the transmitter to the receiver in the form of a bulk wave with pressure p, which propagates through the fluid, and guided waves with von Mises stress σ_{mises}, which travel around the circumference of the cylindrical shell wall. In Fig. 1, the maximum values of pressure and von Mises stress scale with the excitation voltage and follow $2p_0 \approx \sigma_{\max}$. The ToF required for each acoustic wave to travel from the transmitter to the receiver is dependent on the total distance traveled and the sound speed. The bulk wave propagates directly through the cylindrical shell wall, across the fluid, and through the opposing wall before being detected by the receiver. Thus, the bulk wave ToF T_b is calculated as

$$T_b = \frac{2h}{c_l} + \frac{2a}{c_f} \tag{1}$$

where c_l is the longitudinal sound speed in the cylindrical shell and c_f is the sound speed in the fluid. Here c_l and c_f are dependent on the material properties of the cylindrical shell and fluid, respectively, and the environmental conditions such as temperature, but their dependence on the frequency of the acoustic wave is negligible compared to other effects such as dispersion in the cylindrical shell wall. Similarly, the ToF T_g of the guided waves is calculated as

$$T_g(f) = \frac{\pi\left(a + \frac{1}{2}h\right)}{c_g(f)} \tag{2}$$

where $c_g(f)$ is the group velocity of the guided waves, which is dependent on the frequency of the acoustic wave f, the cylindrical shell geometry and material properties, and the environmental conditions such as temperature. The group velocity of the guided waves within a cylindrical shell are obtained from the dispersion curves, which relate the acoustic wavenumber and frequency by solving the equations of motion and boundary conditions in the cylindrical shell. We compute the dispersion curves using the global matrix method presented by Qu *et al.* [22], [23]. This method involves representing the waves within the cylindrical shell in terms of displacement potentials with radial components

$$\varphi(r) = A_1 J_{\text{kb}}\left(\frac{\omega r}{c_l}\right) + A_2 Y_{\text{kb}}\left(\frac{\omega r}{c_l}\right) \tag{3a}$$

$$\psi(r) = A_3 J_{\text{kb}}\left(\frac{\omega r}{c_s}\right) + A_4 Y_{\text{kb}}\left(\frac{\omega r}{c_s}\right) \tag{3b}$$

where A_1, A_2, A_3, and A_4 are unknown coefficients and $J_{\text{kb}}(\cdot)$ and $Y_{\text{kb}}(\cdot)$ are (kb)th order Bessel functions of the first and second kinds, respectively. Next neglecting the fluid loading on the cylinder surfaces results in zero compressional and shear stresses, where these stresses relate to the displacement potentials according to Hooke's Law. This yields four equations (zero compressional stress at $r = a$ and b and zero shear stress at $r = a$ and b). Thus, for every combination of (k, f), we obtain a linear system with four equations and four unknowns (A_1, A_2, A_3, and A_4). We identify guided wave modes as combinations (k, f) for which the linear system is singular. This results in one curve $k(f)$ for each guided wave mode. Finally, for each guided wave mode, we calculate the dispersion curve in terms of the group velocity

$$c_g(f) = 2\pi \frac{df(k)}{dk}. \tag{4}$$

For a full derivation of the dispersion curve computation, see Qu *et al.* [22], [23].

Fig. 2 shows the dispersion curve for an empty 6061 aluminum cylindrical shell with longitudinal sound velocity $c_l = 6420$ m/s, shear sound velocity $c_s = 3040$ m/s, inner diameter $2a = 114.3$ mm, and thickness $h = 5.8$ mm, where we have assumed no loading (traction free) on the inner/outer boundaries. We label the different guided wave modes 1–9. We observe that the group velocity of most wave modes is zero at low frequencies; and as the frequency increases, the group velocity rapidly increases, and then drops down before approaching the shear sound speed in the cylindrical shell. As a result, a broadband excitation signal will be distorted as different frequency components propagate at different speeds. This dispersive behavior has been exploited previously, e.g., to determine the resonance behavior of structures via chirp excitations [28] or detect structural damage [29].

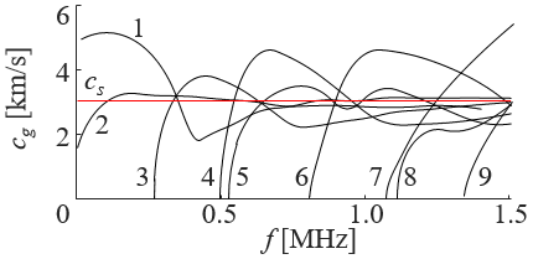

Fig. 2. Dispersion curve for an empty cylindrical shell. The group velocity of several guided wave modes is plotted as a function of frequency with the shear sound speed c_s (red) indicated for reference.

III. Methods

We use the experimental setup illustrated in Fig. 1, with a 6061 Al cylindrical shell of inner diameter $2a = 114.3$ mm and thickness $h = 5.8$ mm, equipped with an opposing piezoelectric transmitter/receiver (PZT-5J, resonance frequency 0.3 MHz, STEMiNC). The transmitter is driven by a function generator (Tektronix AFG 3102) with 10V amplitude, and the receiver is connected to an oscilloscope (Tektronix DPO 7054C) after being filtered (low-pass, 2 MHz) and amplified (20 dB; Krohn-Hite Model 3945 Digital Programmable Filter). We excite the transmitter with a linear chirp signal $s_0(t)$ modulated by a Tukey window function $W(t)$ to analyze the effect of center frequency f_c, frequency bandwidth Δf, and chirp duration T of the signal independently. The input signal is given as

$$s_0(t) = W(t)\sin\left[2\pi\left(f_c - \frac{1}{2}\Delta f\right)t + \frac{\pi}{T}\Delta f t^2\right] \tag{5}$$

where the Tukey window function is defined as

$$W(t) = \begin{cases} \frac{1}{2}[1 - \cos(4\pi t/T)] & \text{for } 0 \le t \le T/4 \\ 1 & \text{for } T/4 \le t \le 3T/4 \\ \frac{1}{2}[1 - \cos(4\pi(T-t)/T)] & \text{for } 3T/4 \le t \le T. \end{cases} \tag{6}$$

After exciting the transmitter, we measure the receiver response $s(t)$. To detect the arrival time of the bulk wave, we cross correlate (CC) the measured signal with the excitation chirp

$$CC(t) = \int_{-\infty}^{\infty} s(\tau)s_0(\tau + t)d\tau \tag{7}$$

and calculate the CC envelope (CCE) based on the Hilbert transform,

$$\text{CCE}(t) = \left|CC(t) + i\frac{1}{\pi}\int_{-\infty}^{\infty}\frac{CC(\tau)}{t-\tau}d\tau\right| \tag{8}$$

where $i = \sqrt{-1}$.

Fig. 3(a) shows an example signal $s(t)$ within an air-filled cylindrical shell (red) and a water-filled cylindrical shell (black), and Fig. 3(b) shows the corresponding CCEs.

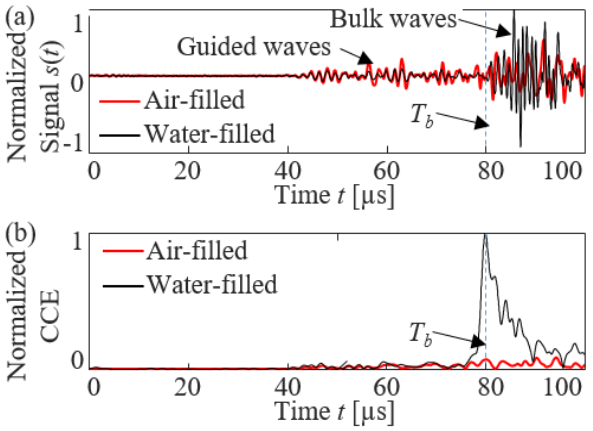

Fig. 3. Measured signal $s(t)$ and corresponding CCE(t) in a fluid-filled cylindrical shell, indicating the theoretical arrival time T_b.

In practice, when the transducer is at rest and then excited with a sinusoidal signal, the resulting acoustic signal builds in amplitude over the duration of the excitation and then decays exponentially due to ringing in the transducer, rather than stopping abruptly [30]. This gradual increase and then decrease in amplitude elongate the transmitted acoustic signal and were found to shift CCE(t) by approximately $T/2$. Thus, to correct this elongation, we shift the CCE(t) by $-T/2$ in time. The experimentally measured arrival time $\hat{T}_b$ is calculated as the time t that maximizes the shifted CCE(t).

From Fig. 3(a), we observe that the addition of fluid in the cylindrical shell reduces the amplitude of the guided waves, but their amplitudes are still on the order of the bulk waves. From Fig. 3(b), we observe that despite the guided and bulk waves having similar magnitude, the CCE amplitude is significantly larger for the bulk waves. This is due to the dispersion of the guided waves, wherein different frequency components of the chirp signal travel at different speeds, expanding or contracting the chirp signal. This then reduces the CC between the input signal with linearly increasing frequency and the measured signal with distorted frequencies. This process is akin to a matched filter, where the filter is designed to pass bulk waves and reject guided waves.

IV. Results and Discussion

To determine the effect of the broadband excitation on the guided waves, we measure the CCE amplitude of the guided waves alone (no bulk wave) by exciting the empty cylindrical shell with linear chirps of duration $T = 10$ μs, center frequency $f_c \epsilon [0.1, 1.5]$ MHz, and bandwidth $\Delta f \epsilon [0.1, 1.0]$ MHz. Fig. 4 shows the maximum CCE amplitude measured by the receiver for the empty cylindrical shell as a function of f_c and Δf. We observe large CCE amplitudes for center frequencies approaching $f_c = 0.35$, 0.60, 1.10, and 1.65 MHz. We observe in Fig. 2 that near $f_c = 0.35$ MHz, the propagation is dominated by Modes 1–3, which have high radial displacement amplitudes. Additionally, $f_c = 0.60$, 1.10, and 1.65 MHz corresponds approximately with longitudinal resonances in the cylindrical shell wall, which results in constructive wave interference that increases the wave amplitude. Finally, we observe that at all center frequencies,

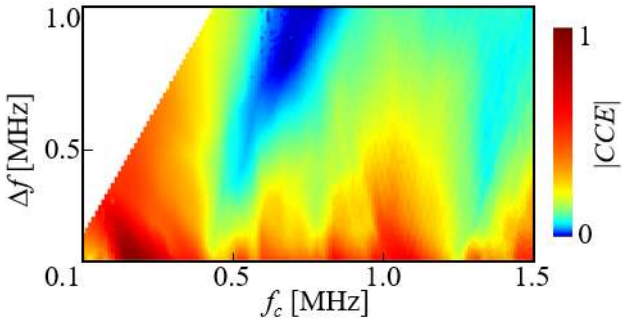

Fig. 4. Measured CCE of the guided waves as a function of center frequency f_c and bandwidth Δf.

increasing the bandwidth reduces CCE amplitude of the guided waves. This occurs because the broadband guided waves experience more distortion (elongation/contraction) due to different frequency components of the linear chirp propagating at different group velocities. This indicates the feasibility of using broadband excitation to mitigate interference between detected bulk waves in the presence of guided waves.

To quantify the performance of the technique for measuring the sound speed of a fluid, we implement the ToF measurement technique described in Section III with the water-filled cylindrical shell. We characterize the ToF measurement technique using three metrics.

1) The ToF error between the measured and theoretical arrival times, i.e., ToF error $= |\hat{T}_b - T_b|/T_b$.
2) The SNR, where SNR $=$ CCE$(\hat{T}_b)$/mean(CCE$(|t - \hat{T}_b| > T/2)$) represents the amplitude of the initial bulk wave, compared to the mean amplitude of other waves such as the guided waves and reflections of the bulk wave that arrive more than $T/2$ before or after the measured ToF.
3) The resolution, which is related to the width of the CCE arrival peak, and thus, determines the minimum time-spacing between arrivals from the initial bulk wave, guided waves, and/or reflected bulk waves that can be distinguished. We measure the resolution based on the full-width-at-half-maximum (FWHM) of the CCE peak, nondimensionalized by the center frequency.

Fig. 5 shows the arrival time measurement metrics for a water-filled aluminum cylindrical shell, for which (1) gives a theoretical ToF of $T_b = 78.1$ μs. We calculate (a) the ToF error, (b) the SNR, and (c) the resolution of the measurement technique as a function of the center frequency f_c and bandwidth Δf of the chirp excitation signal. Additionally, we indicate four points (d)–(g) that correspond to Fig. 5(d)–(g), which show the measured signal (solid black) and CCE (dashed red) for several characteristic regions of (f_c, Δf) values. Based on the CCE peaks, we measure arrival times and bulk sound speeds of 113.8 μs and 1020.9 m/s [Fig. 5(d)], 78.2 μs and 1495.9 m/s [Fig. 5(e)], 78.5 μs and 1490.1 m/s [Fig. 5(f)], and 80.6 μs and 1450.9 m/s [Fig. 5(g)]. For low center frequencies ($f_c < 0.8$ MHz), we observe large ToF errors on the order of 36%–50%. From Fig. 5(d), we observe that there is a chirp arrival at approximately the theoretical arrival time T_b, but there is also a high-amplitude

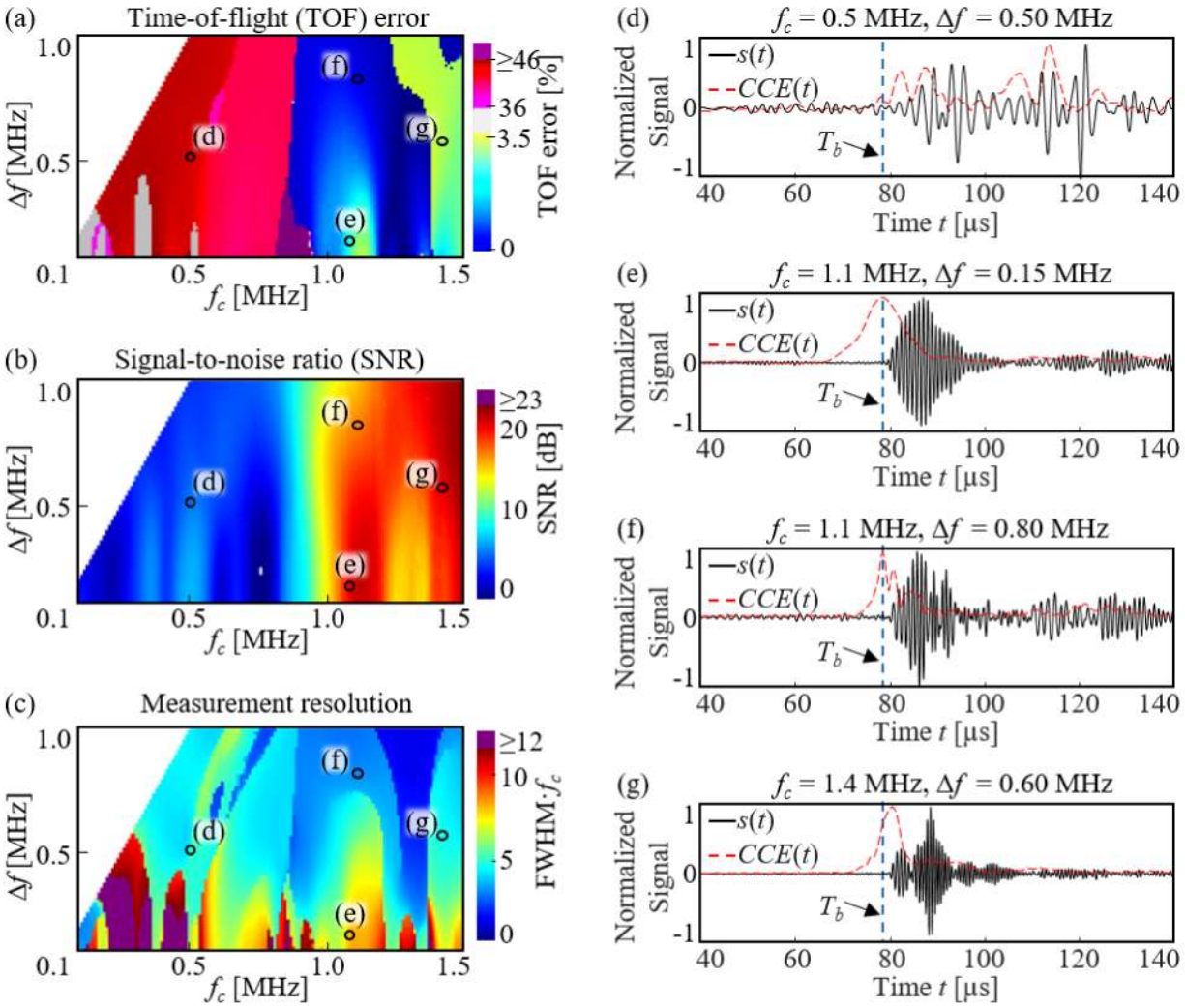

Fig. 5. (a)–(c) Arrival time metrics for the noninvasive acoustic measurements in a cylindrical shell. Metrics include (a) ToF error, (b) signal-to-noise (SNR), and (c) measurement resolution, represented as the product of the FWHM and the center frequency f_c as a function of f_c and bandwidth Δf. (d)–(g) Example measurement signals $s(t)$ and cross correlation envelopes CCE(t) for selected (f_c, Δf) combinations.

wave arriving at the receiver approximately 35 μs after T_b, which results in the large ToF error. To identify the source of the high-amplitude chirp, we have simulated the wave propagation using a 2-D finite element model (COMSOL). The simulation involves exciting a piezoelectric transmitter with a linear chirp voltage and then measuring the pressure within the fluid and the von Mises stress within the cylindrical shell walls. Fig. 6 shows the time snapshots of the propagating waves in terms of pressure p in the fluid and von Mises stress σ_{mises} at times (a) $t < T_b$ and (b) $t \approx T_b$. We observe that the bulk wave propagating through the fluid splits into a center wave and two high-amplitude side waves [Fig. 6(a)]. At $t \approx T_b$, the central wave is measured by the receiver and the side waves enter into the cylindrical shell walls [Fig. 6(b)] where they are guided to the receiver, resulting in the late chirp measurement. This splitting behavior occurs largely due to the spreading of the acoustic burst in the fluid at low frequencies. Additionally, low attenuation of the guided waves at low frequencies yields large vibration amplitudes along the fluid–cylinder interface. As a result, the bulk wave in the fluid is excited by a wide area of the internal cylinder wall instead of a small patch near the transmitter. We note that for the selected dimensions and materials, the split wave dominates the bulk arrival for center frequencies below approximately 0.8 MHz, as indicated in Fig. 5(a) and (b). Above this center frequency, the wave splitting still occurs, but the split waves become less prominent as more energy is focused into the center beam. Finally, Fig. 5(e) shows the response for a higher center frequency near a thickness resonance of the cylindrical shell wall ($f_c = 1.1$ MHz $\approx c_l/h$) and a low bandwidth ($\Delta f = 0.15$ MHz). At this (f_c, Δf) combination, we measure low ToF error [Fig. 5(a)] and high SNR [Fig. 5(b)] but a poor resolution [Fig. 5(c)]. This is due to the chirp resonating as it passes through the walls to/from the fluid. This resonance results in constructive interference that amplifies the bulk wave, which increases the SNR. However, the resonance also results in ringing within the wall, which elongates the chirp and reduces the time resolution. Thus, the increased SNR will reduce the effect of the guided waves, but the decreased resolution will inhibit distinguishing between chirp arrivals

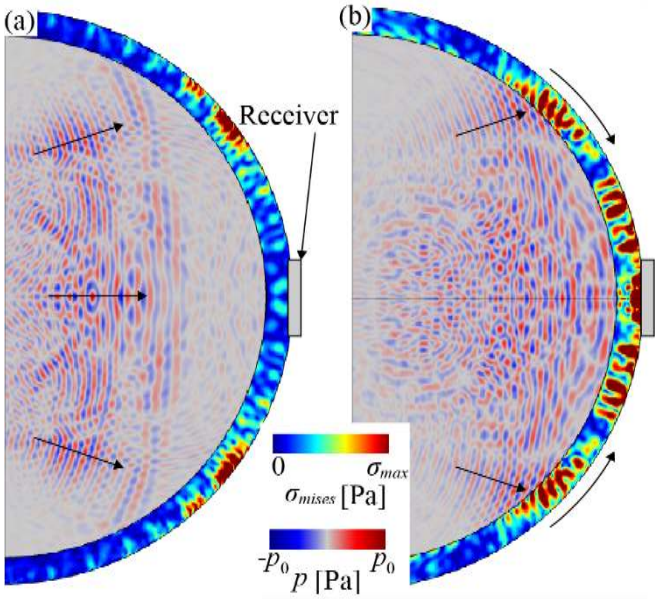

Fig. 6. Snapshots of the time-domain pressure p in the fluid and von Mises stress σ_{mises} for excitation signal with low center frequency $f_c = 0.5$ MHz captured at times (a) $t < T_b$ and (b) $t \approx T_b$.

at similar times due to multiple transmissions or reflections from any objects suspended within the fluid. Alternatively, we observe that using $f_c = 1.1$ MHz $\approx c_l/h$ and increasing the bandwidth to $\Delta f = 0.8$ MHz [Fig. 5(f)] reduces the number of periods where the chirp excites the wall resonance. This results in low ToF error and good resolution, at the cost of a slight reduction in SNR. Additionally, from Fig. 5(a)–(c), we observe that near point (f), there is a larger range of (f_c, Δf) values where the ToF error, SNR, and resolution remain approximately constant. This increases the robustness of the measurement technique when the cylindrical shell dimensions and material parameters are not known with a high degree of accuracy. Finally, Fig. 5(g) shows the measured signals for $f_c = 1.4$ and $\Delta f = 0.60$ MHz. We observe that the measured signal includes two bursts that begin at approximately T_b and $T_b + T$, respectively. We note that the second burst has higher amplitude and is dominated by a 1.55 MHz signal, which approximately coincides with a predicted thickness resonance in the cylindrical shell wall. As a result, the resonance amplifies the 1.55 MHz portion of the signal and causes it to ring and elongate, which delays the time where the peak CCE occurs, and, thus, introduces ToF error. This observation indicates that the ideal combination of (f_c, Δf) values should be selected such that the start or end frequency of the linear chirp does not coincide with a wall thickness resonance frequency.

The results shown in Fig. 4 indicate that broadband excitation of fluid-filled cylindrical shells reduces the amplitude of the guided waves due to increased dispersion. Additionally, from Fig. 5 we observe that an excitation signal with center frequency close to a thickness resonance in the cylindrical shell wall ($f_c \approx c_l/h$) and a bandwidth approximately equal to the center frequency results in the best combination of small ToF error and increased SNR and resolution. We note that different cylindrical shell dimensions and/or material properties will affect the guided wave dispersion curves. Thus, prior knowledge of the cylindrical shell is required to identify a desirable center frequency and bandwidth. Additionally, increasing frequency increases the attenuation within the bulk wave, which may reduce the efficacy of the technique within highly attenuating fluids. Increasing the chirp time results in longer periods of ringing due to resonance within the cylindrical shell walls, and it increases the overlap between the guided and bulk waves. This increases the FWHM, which reduces the measurement resolution. Alternatively, reducing the duration T will increase the bandwidth of the signal. From Fig. 5(g), we observe that if the start or end frequency of the chirp coincides with a wall thickness resonance, the CCE peak will be delayed in time, which introduces error in the ToF measurement. In this article, we select a linear chirp excitation to enable adjusting the center frequency and bandwidth independent of the chirp duration. There is a wide array of alternative signal types such as exponential chirps, Gaussian bursts, etc. with broad frequency bandwidth that are currently being explored as a means of overcoming guided wave interference when performing acoustic measurements in a fluid-filled cylindrical shell.

V. Conclusion

We present a technique for performing noninvasive acoustic ToF measurements of a fluid within a cylindrical shell, which is challenging due to the interference between the bulk wave propagating through the fluid and the guided waves propagating around the cylindrical shell walls. We employ a linear chirp excitation and CC to exploit the dispersion phenomenon of the guided waves, wherein waves with different frequencies arrive at different times. As a result, the guided waves become distorted as different frequency components arrive early or late, while the bulk wave remains unperturbed. We characterize the measurement technique as a function of the excitation center frequency and bandwidth. At low center frequencies, we observe a phenomenon where the bulk wave splits into one component that propagates along the transmitter centerline and two components that propagate away from the centerline until they reenter the cylinder walls and propagate to the receiver as guided waves. This results in a large degree of interference, inhibiting the bulk wave arrival measurement. Alternatively, we observe that using center frequency equal to a thickness resonance in the cylindrical shell wall and a bandwidth approximately equal to the center frequency results in negligible ToF error, high signal-to-noise-ratio, and good measurement resolution. As a result, this technique offers a simple noninvasive technique for measuring the sound speed of a fluid within a closed cylindrical shell or pipe. This ability finds application in a wide range of fields including industrial process control, biomedical monitoring, and material characterization.

References

[1] D. N. Sinha, K. Springer, W. Han, D. Lizon, and S. Kogan, "Applications of swept-frequency acoustic interferometer for nonintrusive detection and identification of chemical warfare compounds," Los Alamos National Lab., Los Alamos, NM, USA, Tech. Rep. LA-UR-97-3113; CONF-970962, Dec. 1997, doi: 10.2172/555542.

[2] Remenieras, Cervenka, and Alais, "Non intrusive measurements of the acoustic pressure and velocity fluctuations of fluids flowing in pipes," in *Proc. IEEE Ultrason. Symp. (ULTSYM)*, Cannes, France, Oct./Nov. 1994, pp. 1323–1326, doi: 10.1109/ULTSYM.1994.401836.

[3] C.-C. Shen, M.-Y. Weng, J.-K. Sheu, Y.-T. Yao, and C.-K. Sun, "*In situ* monitoring of chemical reactions at a solid–water interface by femtosecond acoustics," *J. Phys. Chem. Lett.*, vol. 8, no. 21, pp. 5430–5437, Nov. 2017, doi: 10.1021/acs.jpclett.7b02384.

[4] R. G. Leisure and F. A. Willis, "Resonant ultrasound spectroscopy," *J. Phys., Condens. Matter*, vol. 9, no. 28, p. 6001, Jul. 1997, doi: 10.1088/0953-8984/9/28/002.

[5] J. Maynard, "Resonant ultrasound spectroscopy," *Phys. Today*, vol. 49, no. 1, p. 26, Jan. 2008, doi: 10.1063/1.881483.

[6] D. N. Sinha, "Noninvasive identification of fluids by swept-frequency acoustic interferometry," U.S. Patent 5 767 407 A, Jun. 16, 1998.

[7] M. Fatemi and J. F. Greenleaf, "Application of radiation force in noncontact measurement of the elastic parameters," *Ultrason. Imag.*, vol. 21, no. 2, pp. 147–154, Apr. 1999, doi: 10.1177/016173469902100205.

[8] F. G. Mitri, P. Trompette, and J.-Y. Chapelon, "Detection of object resonances by vibro-acoustography and numerical vibrational mode identification," *J. Acoust. Soc. Amer.*, vol. 114, no. 5, p. 2648, 2003, doi: 10.1121/1.1616921.

[9] L. Flax, L. R. Dragonette, and H. Überall, "Theory of elastic resonance excitation by sound scattering," *J. Acoust. Soc. Amer.*, vol. 63, no. 3, pp. 723–731, Mar. 1978, doi: 10.1121/1.381780.

[10] H. Überall and H. Huang, "Acoustical response of submerged elastic structures obtained through integral transforms," in *Physical Acoustics*, vol. 12. Amsterdam, The Netherlands: Elsevier, 1976, pp. 217–275.

[11] B. J. Zadler, J. H. L. Le Rousseau, J. A. Scales, and M. L. Smith, "Resonant ultrasound spectroscopy: Theory and application," *Geophys. J. Int.*, vol. 156, no. 1, pp. 154–169, Jan. 2004, doi: 10.1111/j.1365-246X.2004.02093.x.

[12] J. Diarmuid Murphy, J. George, and H. Überall, "Isolation of the resonant component in acoustic scattering from fluid-loaded cylindrical shells," *Wave Motion*, vol. 1, no. 2, pp. 141–147, Apr. 1979, doi: 10.1016/0165-2125(79)90016-7.

[13] G. C. Gaunaurd and A. Akay, "Isolation of the spectrograms and rosettes of insonified sets of submerged, concentric, thin shells," *J. Vib. Acoust.*, vol. 116, no. 4, pp. 573–577, Oct. 1994, doi: 10.1115/1.2930466.

[14] F. G. Mitri, J. F. Greenleaf, Z. E. A. Fellah, and M. Fatemi, "Investigating the absolute phase information in acoustic wave resonance scattering," *Ultrasonics*, vol. 48, no. 3, pp. 209–219, Jul. 2008, doi: 10.1016/j.ultras.2008.01.002.

[15] P. Rembert, A. Cand, P. Pareige, M. Talmant, G. Quentin, and J. Ripoche, "The short pulse method of isolation and identification of resonances: Comparison with a quasiharmonic method and application to axisymmetrical scatterers," *J. Acoust. Soc. Amer.*, vol. 92, no. 6, pp. 3271–3277, Dec. 1992, doi: 10.1121/1.404177.

[16] S. M. Kay, *Fundamentals of Statistical Processing: Estimation Theory*, vol. 1. Upper Saddle River, NJ, USA: Prentice-Hall, 1993.

[17] D. C. Gazis, "Three-dimensional investigation of the propagation of waves in hollow circular cylinders. I. Analytical foundation," *J. Acoust. Soc. Amer.*, vol. 31, no. 5, pp. 568–573, May 1959, doi: 10.1121/1.1907753.

[18] D. C. Gazis, "Three-dimensional investigation of the propagation of waves in hollow circular cylinders. II. numerical results," *J. Acoust. Soc. Amer.*, vol. 31, no. 5, pp. 573–578, May 1959, doi: 10.1121/1.1907754.

[19] A. Marzani, "Time–transient response for ultrasonic guided waves propagating in damped cylinders," *Int. J. Solids Struct.*, vol. 45, nos. 25–26, pp. 6347–6368, Dec. 2008, doi: 10.1016/j.ijsolstr.2008.07.028.

[20] J. J. Ditri and J. L. Rose, "Excitation of guided elastic wave modes in hollow cylinders by applied surface tractions," *J. Appl. Phys.*, vol. 72, no. 7, pp. 2589–2597, Oct. 1992, doi: 10.1063/1.351558.

[21] M. Mitra and S. Gopalakrishnan, "Guided wave based structural health monitoring: A review," *Smart Mater. Struct.*, vol. 25, no. 5, May 2016, Art. no. 053001, doi: 10.1088/0964-1726/25/5/053001.

[22] J. Qu, Y. Berthelot, and Z. Li, "Dispersion of guided circumferential waves in a circular annulus," in *Review of Progress in Quantitative Nondestructive Evaluation*, vol. 15. 1996, pp. 169–176, doi: 10.1007/978-1-4613-0383-1_21.

[23] G. Liu and J. Qu, "Guided circumferential waves in a circular annulus," *J. Appl. Mech.*, vol. 65, no. 2, pp. 424–430, Jun. 1998, doi: 10.1115/1.2789071.

[24] K. Xu, D. Ta, P. Moilanen, and W. Wang, "Mode separation of lamb waves based on dispersion compensation method," *J. Acoust. Soc. Amer.*, vol. 131, no. 4, pp. 2714–2722, Apr. 2012, doi: 10.1121/1.3685482.

[25] X. Li and Z. Song, "An ultrasound-based liquid pressure measurement method in small diameter pipelines considering the installation and temperature," *Sensors*, vol. 15, no. 4, pp. 8253–8265, Apr. 2015, doi: 10.3390/s150408253.

[26] V. K. Chillara, B. T. Sturtevant, C. Pantea, and D. N. Sinha, "Ultrasonic sensing for noninvasive characterization of oil-water-gas flow in a pipe," in *Proc. AIP Conf.*, vol. 1806, 2017, Art. no. 090014.

[27] V. K. Chillara, B. Sturtevant, C. Pantea, and D. N. Sinha, "A physics-based signal processing approach for noninvasive ultrasonic characterization of multiphase oil-water-gas flows in a pipe," *IEEE Trans. Ultrason., Ferroelectr., Freq. Control*, early access, Sep. 25, 2020, doi: 10.1109/TUFFC.2020.3026071.

[28] J. E. Michaels, S. J. Lee, A. J. Croxford, and P. D. Wilcox, "Chirp excitation of ultrasonic guided waves," *Ultrasonics*, vol. 53, no. 1, pp. 265–270, Jan. 2013, doi: 10.1016/j.ultras.2012.06.010.

[29] J. E. Michaels and T. E. Michaels, "Detection of structural damage from the local temporal coherence of diffuse ultrasonic signals," *IEEE Trans. Ultrason., Ferroelectr., Freq. Control*, vol. 52, no. 10, pp. 1769–1782, Oct. 2005, doi: 10.1109/TUFFC.2005.1561631.

[30] M. Umeda, K. Nakamura, and S. Ueha, "The measurement of high-power characteristics for a piezoelectric transducer based on the electrical transient response," *Jpn. J. Appl. Phys.*, vol. 37, no. 9B, pp. 5322–5325, Sep. 1998, doi: 10.1143/JJAP.37.5322.

John Greenhall (Member, IEEE) received the B.S. and Ph.D. degrees in mechanical engineering with an emphasis on robotics from the University of Utah, Salt Lake City, UT, USA, in 2012 and 2017, respectively.

From 2016 to 2017, he worked as a Graduate Researcher in conjunction with the NASA Langley Research Center, Hampton, VA, USA, where he researched tailoring material microstructures using ultrasound to organize nano- and microparticles into user-specified patterns that are then fixated in place via stereolithography. He worked with the Los Alamos National Laboratory as a Post-Doctoral Researcher from 2017 to 2019, and as a Research Scientist from 2019 to present. He has authored over 11 journal publications. His research interests include experimental and theoretical acoustics, optimization, signal and image processing, and machine learning.

Dr. Greenhall awards include the NASA Space Technology Research Fellowship and the Distinguished Dissertation Award from The University of Utah Department of Mechanical Engineering.

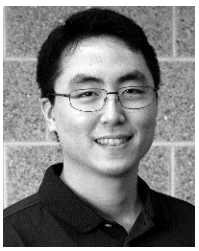

Christopher Hakoda (Member, IEEE) received the B.S. degree in mechanical engineering from the Rose–Hulman Institute of Technology, Terre Haute, IN, USA, in 2014 and the M.S. and Ph.D. degrees in engineering science and mechanics from the Pennsylvania State University in University Park, State college, PA, USA, in 2019.

He is currently a Postdoc Research Associate with the Los Alamos National Laboratory, Los Alamos, NM, USA, and works with the Acoustics and Sensors group on academic- and industry-focused projects. His research focused on fundamental elastodynamic guided wave theory and applied that knowledge to nondestructive evaluation and testing.

Dr. Hakoda started in the Fall of 2019 and is a member of several professional societies including the IEEE TRANSACTIONS ON ULTRASONICS, FERROELECTRICS, AND FREQUENCY CONTROL and the American Physical Society.

Eric S. Davis (Member, IEEE) was born in San Antonio, TX, USA, in 1991. He received the B.S. degree in physics and mathematics from Texas Christian University, Fort Worth, TX, in 2014, and the Ph.D. degree in physics from the University of Houston, Houston, TX, in 2018.

Since 2013, he has been working at the Los Alamos National Laboratory, Los Alamos, NM, USA, first as an Undergraduate Research Assistant, then as a Graduate Research Assistant, and finally as a Postdoctoral Research Assistant starting in 2019. His research focuses both on the fundamental side of physical acoustics (resonant ultrasound spectroscopy and through-transmission for materials characterization) and on instrumentation and experimental design for the development of acoustic sensors.

Dr. Davis is a member of the IEEE TRANSACTIONS ON ULTRASONICS, FERROELECTRICS, AND FREQUENCY CONTROL (IEEE-UFFC) as well as the Acoustical Society of America (ASA).

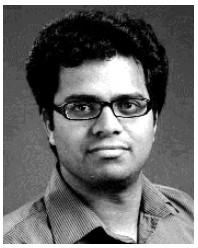

Vamshi Krishna Chillara (Senior Member, IEEE) received the bachelor's degree in mechanical engineering from the Indian Institute of Technology Madras, Chennai, India, in 2010, and the Ph.D. degree in engineering science and mechanics from The Pennsylvania State University, University Park, State College, PA, USA, in 2015.

He is currently a Research Scientist with the Acoustics and Sensors Team, Los Alamos National Laboratory, Los Alamos, NM, USA, where he has been since October 2015. His research interests include the development of ultrasonic sensors and sensing methodologies for a wide variety of structural, chemical, and biomedical applications. He has authored over 30 journal and conference publications and has three invention disclosures to date.

Cristian Pantea (Senior Member, IEEE) was born in Romania in 1972. He received the B.Sc. and M.Sc. degrees in physics from the University of Cluj, Cluj-Napoca, Romania, in 2005 and 2006, respectively. He received the Ph.D. degree in physics from Texas Christian University, Fort Worth, TX, USA, in 2004.

Since 2000, he has been working at the Los Alamos National Laboratory, Los Alamos, NM, USA, as a Graduate Student, Post-Doctoral Research Associate, and, lately, as a Research Scientist. His research focuses on different acoustics techniques for materials characterization (pulse-echo, resonant ultrasound spectroscopy, swept-frequency acoustic interferometry, and acoustic nonlinearity) and the development of acoustic sensors and methods with applications in both applied and fundamental research.

Dr. Pantea is a member of the IEEE TRANSACTIONS ON ULTRASONICS, FERROELECTRICS, AND FREQUENCY CONTROL (IEEE-UFFC0), the Acoustical Society of America (ASA), and the American Physical Society (APS). He is a reviewer for several journals, including IEEE TRANSACTIONS ON ULTRASONICS, FERROELECTRICS, AND FREQUENCY CONTROL, *Applied Physics Letter and Ultrasonics*.